PROCEEDINGS, TOUGH Symposium 2006
Lawrence Berkeley National Laboratory, Berkeley, California, May 15–17, 2006

MODELING ORGANIC SPILLS IN COASTAL SITES WITH TMVOC V.2.0

Alfredo Battistelli

RISAMB Dept., INFRAMB Div., Snamprogetti SpA (ENI Group)
Via Toniolo 1, Fano (PU), 61032, Italy
e-mail: alfredo.battistelli@snamprogetti.eni.it

ABSTRACT

Contaminant spills are frequently encountered in coastal sites where many industrial plants are located. Among them, refineries and petrochemical plants are often built close to the sea for easy transport of crude oil and final by-products. The migration of organic compounds spilled in the subsurface of coastal sites can be influenced by the effects of sea water intrusion in the aquifers discharging to the sea.
An improved version of TMVOC numerical simulator can model the migration of multi-component organic mixtures under multiphase conditions accounting for the effects of sodium chloride dissolved in the aqueous phase on thermophysical properties of groundwater, following the basic approach used for saline brines in the EWASG module. The thermodynamic formulation is introduced, together with main hypotheses and assumptions.
Then, simulations of a multi-component organic spill using a 2D vertical numerical model are presented to show main code capabilities and to highlight the effects of sea water intrusion on the distribution of contaminants within the aquifer. The effects of the construction of an impervious wall on the NAPL plume migration is also investigated.

INTRODUCTION

Coastal sites contaminated by hydrocarbons and organic solvents are often encountered, as many industrial plants are located close to the coast. In Italy, for instance, many refineries and petrochemical plants are located along the 7400 km of Italian coast (Rusi et al., 2005). The organic contaminants spilled in these sites can reach the sea both as free NAPL and dissolved in the groundwater. The design and implementation of containment and remediation activities in these sites should properly take into account both the processes linked to the 3-phase flow of VOCs mixtures as well as the density driven groundwater flow which controls the extension of sea water intrusion in coastal aquifers. Due to the higher density, the sea water penetrates inside the coastal aquifer at distances from the coast depending on the aquifer thickness, the hydraulic conductivity, and the amount of flow discharged to the sea. The lighter groundwater flows above the sea water intrusion with a concentration of discharged flow in the upper aquifer section. The presence of sea water intrusion can then affect both the migration of VOCs dissolved in the groundwater, as well as that of a NAPL lense migrating at the vadose zone – water table interface.
Whereas 3-phase compositional flow capabilities were already available with TMVOC V.1.0 (Pruess and Battistelli, 2002), the modeling of flow of a salt solution with variable salinity was possible within the TOUGH2 environment using both the EOS7 and EOS7R modules (Pruess, 1981; Oldenburg and Pruess, 1995) and the EWASG module (Battistelli et al., 1997). A first attempt to couple 3-phase flow and density-dependent groundwater flow was made by including the EOS7 brine treatment into the T2VOC code (Sanese et al., 2003). The necessary capabilities are now available within an improved version of TMVOC simulator which can be used to study the migration of organic contaminants in coastal sites under natural as well as anthropically modified flow conditions.

TMVOC VERSION 2.0

TMVOC V.1.0 (Pruess and Battistelli, 2002; 2003) is a numerical simulator developed for 3-phase non-isothermal flow of water, a user-defined set of gaseous species and a mixture of VOCs in 3D heterogeneous porous media. An extension of the TOUGH2 general-purpose simulation program (Pruess et al., 1999), TMVOC was originally designed for applications to contamination problems that involve hydrocarbon fuel or organic solvent spills in the saturated and unsaturated zones.
The main enhancements in TMVOC V.2 relative to V.1 are as follows:

- a new class of compounds, i.e. dissolved solids treated as tracers, is added (Battistelli, 2004); when modeling dissolved solids, the complete disappearance of the aqueous phase cannot be treated.
- organic compounds can be degraded by reactions mediated by microbial populations following a generalized multiple Monod's kinetic law, accounting for the concentration of substrates, electron acceptors and nutrients (Battistelli, 2004).
- all mass components can adsorb on the rock matrix following a generalized adsorption isotherm which can replicate the linear, Freundlich and Langmuir isotherms (Carpita et al; 2006).
- all mass components can optionally decay following a first order kinetic law.

- NaCl can be specified among the dissolved solids; brine thermophysical properties are then computed as a function of NaCl content in the aqueous phase following the EWASG formulation (Battistelli et al., 1997; Aquater, 2003). The halite precipitation is not modeled in the 3-phase version of TMVOC V.2, whereas it can be simulated in a specialized version called TMGAS, developed for the injection of gas mixtures in geological structures (Battistelli et al., 2003).

Moreover, in TMVOC V.2 the thermodynamic calculations are still performed on the more convenient mole fraction basis, but the secondary parameters are stored in array PAR on a mass fraction basis. Mass balance equations are then assembled as made by standard TOUGH2 EOS modules. This allows once again, to use several standard TOUGH2 subroutines where specialized versions are required by V.1.

The mass components tracked by TMVOC V.2. are assumed to be distributed under thermodynamic equilibrium conditions in the three possible flowing phases: gas, aqueous, and NAPL. Any combination of the three phases and related possible phase transitions are modeled by TMVOC V.2 as shown in Fig. 1, with the limitations specified above when dissolved solids are treated. On the other hand, single-gas phase conditions can always be specified for inactive elements to simulate atmospheric boundary conditions often needed for environmental applications. While molecular diffusion is modeled, the mechanical dispersion is not accounted for, as is done in the standard TOUGH2 code.

A detailed description of the thermodynamic and numerical formulations of TMVOC V.1.0, is given by Pruess and Battistelli (2002), whereas the treatment of brine properties as a function of NaCl content derived from the EWASG module is described by Battistelli et al. (1997).

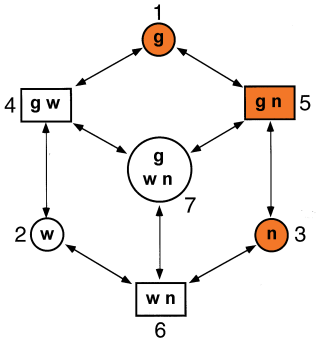

Figure 1. Phase combinations and phase transitions modeled by TMVOC V.2: w, g and n stand for aqueous, gas and NAPL. Shaded phase combinations cannot be modeled when dissolved solids are treated.

Other improvements in the EOS module are as follows:

- the effect of NCGs dissolved in the brine is accounted for when evaluating brine density following the approach suggested by Garcia (2002).
- the NCGs internal data bank has been expanded from the 8 initial gases to 23 in the present version by adding new inorganic gases and hydrocarbons.
- the primary variable tracking the NaCl content in the brine is the salt molality; the NaCl mole fraction in the aqueous phase is computed assuming the salt is completely dissociated, which is a reasonable assumption at the conditions commonly found in coastal site applications.

SIMULATION OF A NAPL SPILL IN A COASTAL SITE

Although the model used is highly simplified, the main hydrogeologic characteristics and the features of the simulated organic spill are derived from those experienced in a coastal site where characterization studies and remediation activities have been performed during the last three decades. The spill takes place at low rates within the vadose zone; it produces a lense of NAPL migrating preferentially in the direction of piezometric gradient. A 2D vertical grid perpendicular to the coastline is used; in this way it is assumed that the NAPL spill takes place along a line parallel to the coast, as could happen with distributed leakages along a buried pipeline or a sewer. The simulated containment works are represented by the construction of a vertical impervious wall parallel to the coastline from the surface to a depth of 5 m bsl. The wall can stop the floating NAPL lense, whereas the aquifer can flow beneath. The VOCs dissolved in the groundwater can still flow to the sea. The modeled impervious wall represents only one of the necessary containment and remediation works. These works can include the recovery of NAPL, the construction of a well barrier for the pumping of contaminated groundwater, and the stopping of NAPL spill.

Conceptual model

The conceptual model is shown in Figure 2. It is a 2D section of 500 m length and 35 m thickness, of which 5 m are above and 30 m below the sea level. The section has a width of 1 m. The spill point is located at coordinates x = 199.5 m e z = + 3.25 m asl. The impervious wall is 1 m wide and is located at x = 99.5, reaching a depth of -5 m asl. The aquifer thickness increases from the right boundary to the coast, where its bottom is 30 m below the sea level. The phreatic aquifer flows from right to left with an average hydraulic gradient of 8E-3 m/m.

The rock domains distribution is shown in Figure 2 and their main petrophysical characteristics are listed in Table 1.

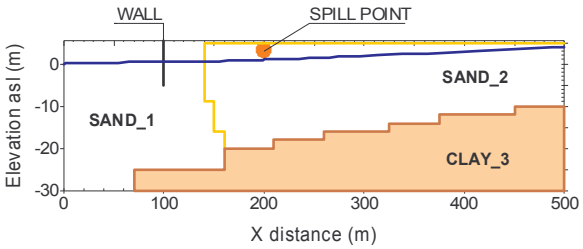

Figure 2. Rock domain distribution on the 2D vertical section. Hydraulic head values of +4 m and 0 m asl are assigned on the right and left boundaries, respectively.

The capillary pressure and relative permeability curves for 3-phase systems are described according to the Parker et al. (1987) and Stone (1970) models, respectively. In particular, for the sand domains the irreducible saturations of gaseous, aqueous and oil phases are 0.01, 0.20, and 0.05 for SAND1, and 0.01, 0.40, and 0.07 for SAND2, respectively.

Table 1. Main characteristics of rock domains.

Domain	Rock type	ρ_R (kg/m^3)	φ	k_{hor} (m^2)	k_{ver} (m^2)	foc
1	Clean sand	2700	0.30	4×10^{-11}	2×10^{-11}	0.001
2	Silty sand	2700	0.30	1×10^{-11}	1×10^{-12}	0.002
3	Silty clay	2700	0.45	1×10^{-15}	1×10^{-16}	0.005

Other two domains are used to fix atmospheric boundary conditions at the grid top and the sea boundary conditions at the left grid side. For this application the formation heterogeneities, the seasonal water table fluctuations and the effects of sea tides have been neglected. A constant meteoric recharge, made up of pure water, was assumed equal to 31.6 and 12.6 mm/year for the clean coastal sands and the silty sands, respectively. A relative humidity of 60% was assigned to the atmospheric boundary elements, which drives a diffusive flux of water vapor from the vadose zone to the atmosphere.

The simulations required several consecutive steps:

- Set up of initial conditions at the lateral left and right boundary columns.
- Steady state of 2D grid, controlled by gravity and capillary forces and subject to the boundary conditions at the lateral and top grid sides, before the construction of the impervious wall.
- Modeling of spill for 5 years in the absence of the wall.
- Modeling of the effects of wall construction performed after 1.5 years of spill. The NAPL migration is modeled for a total spill time of 5 years. It is assumed that wall construction is performed instantaneously.

To show the effects of sea water intrusion, the simulation of spill was performed considering both a salt and a fresh water boundary at the left grid side.

Discretization grid

The vertical section is discretized with 29 layers and 65 columns for a total of 1885 elements. The vertical spacing is 0.5 m above sea level and is progressively increased in the lower section. The horizontal spacing is reduced to a minimum of 1 m at the sea boundary and near the wall and spill point locations.

Simulated scenarios

Three different spill scenarios are discussed:

- **Case A**, assuming fresh water conditions at the sea boundary; a constant NaCl content of 1,000 ppm has been assigned to both aquifer lateral bondaries.
- **Case B**, assuming sea water conditions at the sea boundary; a constant salinity of 36,000 ppm has been assigned to the sea water boundary.
- **Case C**, same boundary conditions of Case B, but with the presence of the impervious wall constructed after 1.5 years of spill.

Modeling of natural states

The initial conditions were determined by running the system to a steady state governed by gravity and capillary equilibrium under the boundary conditions specified before. The only difference between Case A and Cases B-C is that fresh water and sea water boundary conditions are specified for the former and latter cases, respectively. The density and viscosity of the aqueous phase at ambient conditions are listed as a function of NaCl content in Table 2. The sea water density and viscosity are 2.3% and 6.0%, higher than those of groundwater. The piezometric surface representative of steady state (initial) conditions for Cases A and B is shown in Figure 3. The reduction of thickness available for aquifer flow due to sea water intrusion in Case B is responsible for the higher water table elevation close to the sea side. The sea water intrusion at steady state conditions for Case B is shown in Figure 4 where the contouring of NaCl mass fraction is plotted. Sea water can be found at the bottom of the aquifer at more than 100 m from the coastline.

Table 2. Aqueous phase properties at 20°C and 1.013 bar.

Aqueous phase property	Pure water	Aquifer	Sea
NaCl (mg/kg)	0.	1000.	36000.
Density (kg/m^3)	998.3	999.0	1022.1
Viscosity (Pa s)	1.003×10^{-3}	1.004×10^{-3}	1.064×10^{-3}

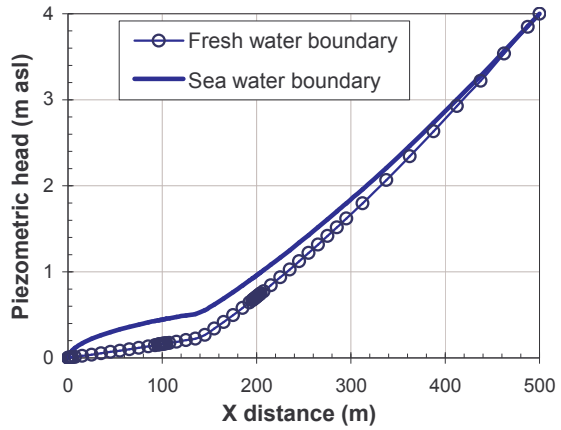

Figure 3. Piezometric head under steady state conditions for cases A and B-C.

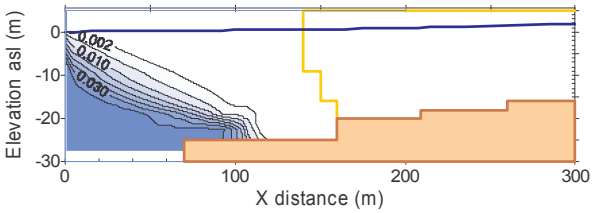

Figure 4. Distribution of sea water intrusion under steady state conditions for Case B.

The confinement of groundwater flow to the upper aquifer section near the coast determines quite different flow profiles, as shown in Figure 5: the groundwater flow towards the sea is concentrated in the upper grid layers for Case B, while it is almost constant over the vertical for Case A. Due to the mixing of sea water into the outflowing groundwater, there is an inflow of sea water to balance the outflow, as shown in Figure 5.

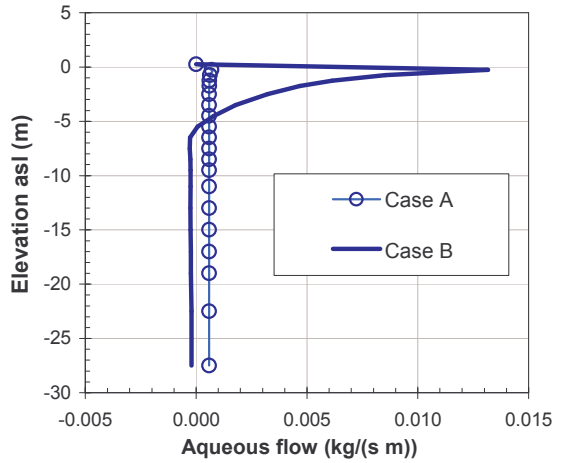

Figure 5. Steady state groundwater flow at sea boundary for Case A and B.

Spill features

The NAPL spill is modeled for 5 years assuming a constant rate of 5.787E-4 kg/s, equivalent to 50 kg/day. The NAPL composition by mass is listed in Table 3 together with the main characteristics of the 6 mixture components considered. Linear adsorption isotherms are assumed for all the VOCs. Main properties of NAPL at ambient conditions are listed in Table 4. They are computed using the TMVOC correlations starting with VOC's properties published by Reid et al. (1987). The molecular diffusion coefficients of all VOCs in the aqueous phase and the NAPL are assumed constant and equal to 6.0E-10 m^2/s. Values ranging from 7.1E-6 to 8.8E-6 m^2/s, at the reference conditions of 0°C and 1.013 bar, are assigned to the VOCs in the gaseous phase. The Millington-Quirk model is used to evaluate the tortuosity effects.

Table 3. Composition of spilled NAPL and properties of mixture components. The saturation pressure is computed at 20°C.

VOC	% mass	MW (g/mol)	Koc (m^3/kg)	Psat (Pa)	Solubility (mg/L)
n-decane	47	142.286	7.000	13	3
benzene	2	78.114	0.089	986	1780
toluene	6	92.141	0.273	291	515
p-xylene	15	106.168	0.550	871	175
n-propylb.	15	120.195	1.050	338	60
n-pentane	15	72.151	0.635	56433	0.4

Table 4. Properties of spilled NAPL at 20°C and 1.013 bar.

NAPL property	Value
Molecular weight (g/mol)	111.729
Density (kg/m^3)	755.40
Dynamic viscosity (Pa s)	0.506×10^{-3}
Vapor pressure (Pa)	13835

Observing the VOCs properties, it can be seen that n-pentane has a strong tendency to the partition into the gas phase; BTEX, mainly benzene and toluene, have a significative solubility in the groundwater, and n-decane has a remarkable tendency to adsorb on organic carbon. The partitioning behaviour of spilled NAPL components, which can be inferred from Table 3, is clearly shown in Figures 6 and 7 below. Figure 6 shows the molar composition of spilled NAPL and the composition of VOCs dissolved in the groundwater at equilibrium with the NAPL: benzene, toluene and p-xylene are clearly the most soluble mixture components. In Figure 7 the relative amount of adsorbed VOCs and of the VOCs present in the gas phase is shown.

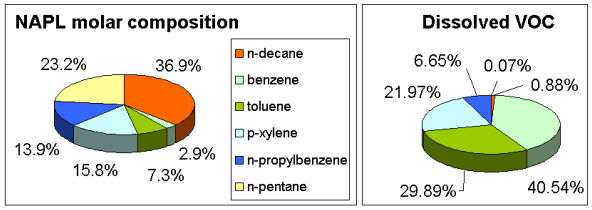

Figure 6. Molar composition of spilled NAPL and VOCs dissolved in pure water at equilibrium.

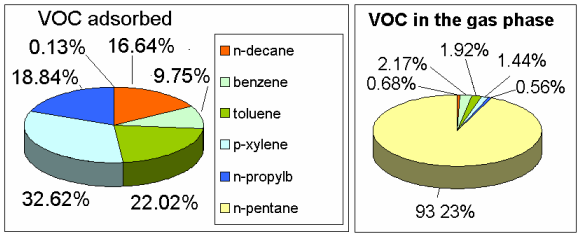

Figure 7. VOCs adsorbed on organic carbon and VOCs in the gas phase at equilibrium with the NAPL.

Case A

The 5-year spill produces the NAPL distribution shown in Figure 8: the lense reaches the sea and free NAPL is discharged outside the model grid. Figure 9 shows the distribution of total VOCs dissolved in the aqueous phase. The maximum, of course, is found where free NAPL is present. Finally the amount of VOCs in the different phases is plotted as a function of time in Figure 10 which clearly shows when the NAPL starts to flow to the sea.

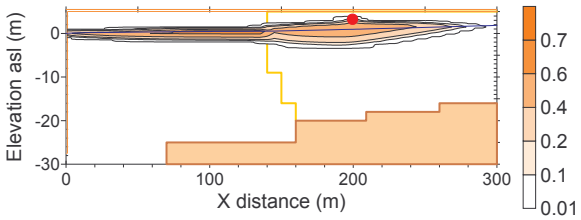

Figure 8. Contouring of NAPL saturation after 5-year spill for Case A.

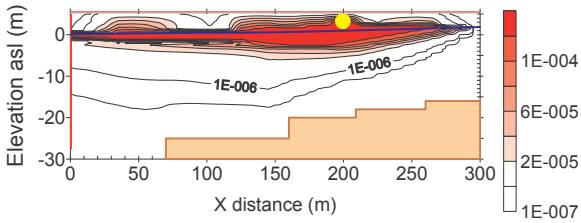

Figure 9. Contouring of dissolved VOCs mass fraction after 5 years of spill for Case A

Case B

The corresponding results obtained after the 5 year-spill for Case B are shown in Figures 11, 12 and 13, respectively. Figure 12 shows that the sea water

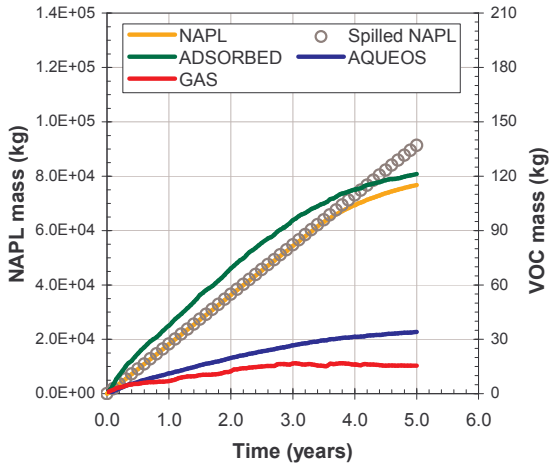

Figure 10. Mass balances of VOCs in the different phases as a function of time for Case A.

intrusion concentrates the flow of dissolved VOCs into the upper aquifer section compared to Case A. Reducing the thickness available for the groundwater flow in the last 120 m close to the sea side, the sea water intrusion reduces the aquifer flow rate and the average aquifer hydraulic gradient upstream. These changes slightly impact the migration of NAPL lense which is affected by the water table gradient.

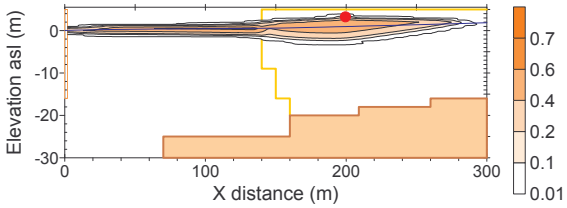

Figure 11. Contouring of NAPL saturation after 5 years of spill for Case B.

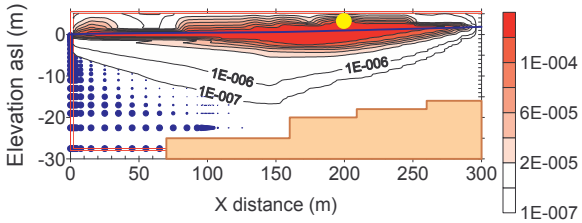

Figure 12. Contouring of dissolved VOCs mass fraction after 5 years of spill for Case B.

Case C

Case C is modeled assuming that the impervious wall is constructed after 1.5 years of spill. Thus, a restart is made taking the conditions computed after 1.5 years for Case B.

The results obtained after 5 years of spill are shown in Figures 14 and 15, whereas Figure 16 presents the simulation results for a simulation time exceeding 6 years.

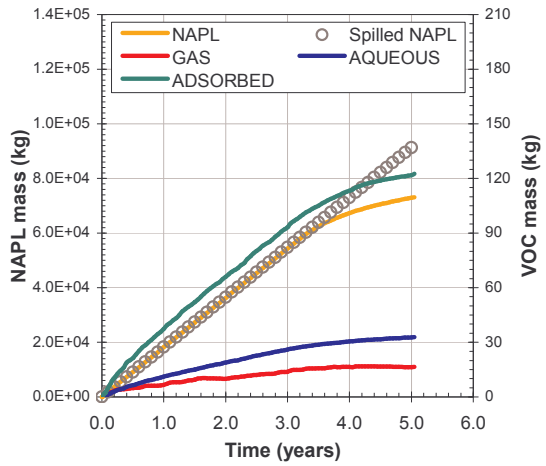

Figure 13. Mass balances of VOCs in the different phases as a function of time for Case B.

This time the NAPL lense migration is completely stopped by the impervious wall so that VOCs can leave the simulation grid only dissolved in the aqueous phase, or due to advective and diffusive flux within the gas phase towards the atmosphere.

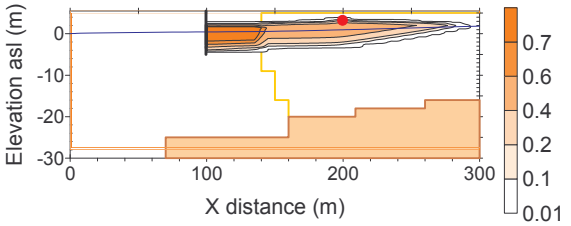

Figure 14. Contouring of NAPL saturation after 5 years of spill for Case C.

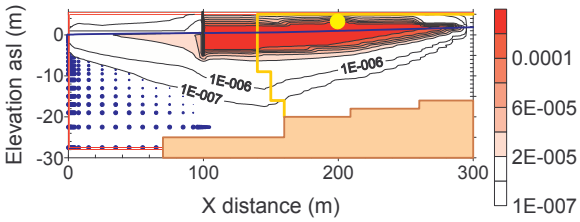

Figure 15. Contouring of dissolved VOCs mass fraction after 5 yearsof spill for Case C.

VOCs flux to the sea

Figure 17 shows the flux of dissolved VOCs at the sea side after 5 years of spill for the 3 simulated cases. The presence of sea water intrusion concentrates the VOCs flux in the upper aquifer section, whereas the contaminants are present at lower depths for Case A, albeit at fairly low concentrations. The impervious wall (Case C) is able to reduce the overall contaminant flux to the sea with respect to Case B, due to the containment of free

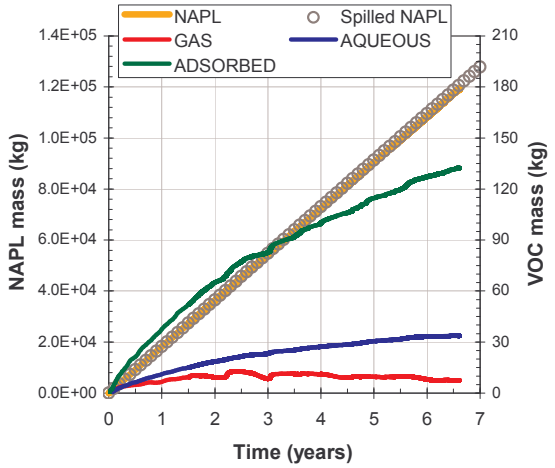

Figure 16. Mass balances of VOCs in the different phases as a function of time for Case C.

NAPL in smaller volumes, which limits the contact between the free NAPL and the groundwater. Thus, the wall actually reduces the advective flow of contaminants in the groundwater. This is shown clearly in Figure 18 where the concentration of VOCs dissolved in the groundwater at an elevation of -0.25 m asl after 5 years of spill is plotted as a function of the distance from the coast. Of course, additional containment works would be needed to further reduce the outflow of contaminants.

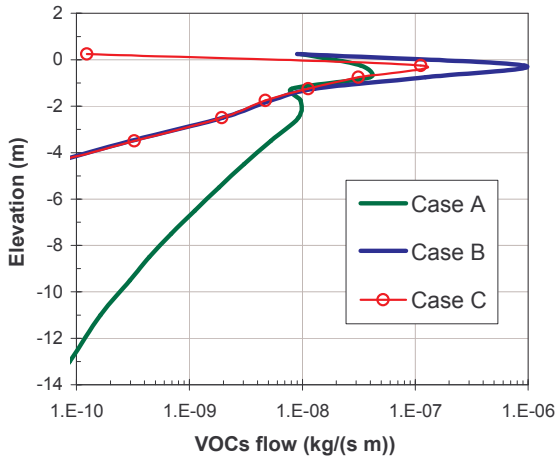

Figure 17. Total VOCs flow in the aqueous phase at the sea boundary after 5 years of spill for Cases A, B and C.

VOCs flux to the atmosphere

The flux of VOCs to the atmosphere is due to both advection and molecular diffusion; the total flux in the gas phase after 5 years of spill is shown for the 3 Cases in Figure 19. The advective flux dominates around the spill point where there is a strong evaporation of n-pentane.

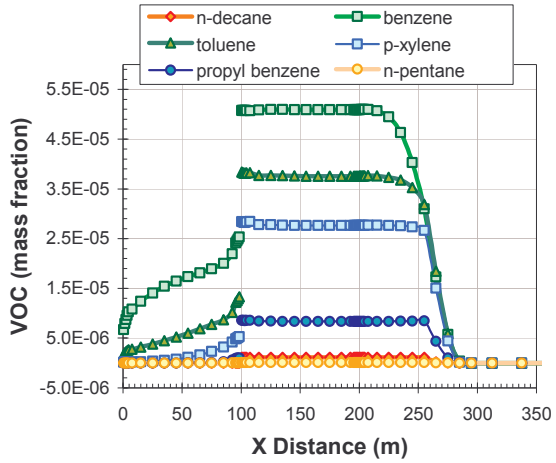

Figure 18. Mass fraction profile of dissolved VOCs after 5 years of spill for Case C at an elevation of -0.25 m asl.

Molecular diffusion is relevant around the spill point as well as at the edge of the NAPL lense, where VOCs vaporize in the interstitial air of vadose zone. For Case C, both advection and diffusion are high upstream of the wall, where the NAPL accumulates. The wall avoids the VOCs flux to the atmosphere downstream of the wall location, but a strong flow is concentrated just upstream of it. This needs to be taken into consideration for the high risk level associated to the possible inhalation of VOC vapors by the personnel on-site.

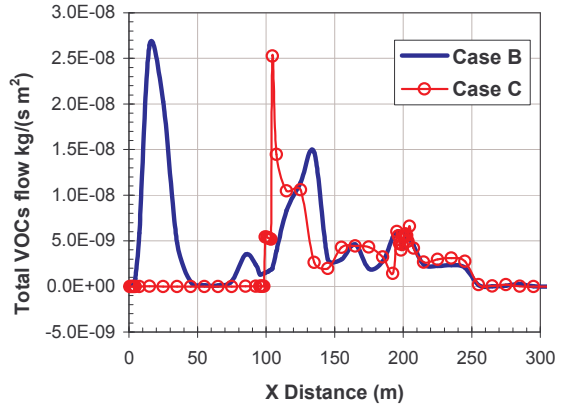

Figure 19. Total VOCs flow in the gas phase towards the atmosphere after 5 years of spill for Cases B and C.

VOCs flowing out of the model grid

The effect of the impervious wall on the migration of individual VOCs is shown for Cases B and C in Figure 20. VOCs are mainly lost for the outflow of NAPL in Case B: this explains why an average of 20% of spilled mass is lost after 5 years of spill. An higher percentage of n-pentane is lost because of the flux to the atmosphere. When the wall is present, no NAPL flow outside the grid is allowed, and VOCs are lost both dissolved in the groundwater and due to the advective and diffusive flux to the atmosphere. Benzene and toluene are lost due to the groundwater flow beneath the impervious wall, whereas n-pentane is lost because of advective and diffusive fluxes in the gas phase within the vadose zone.

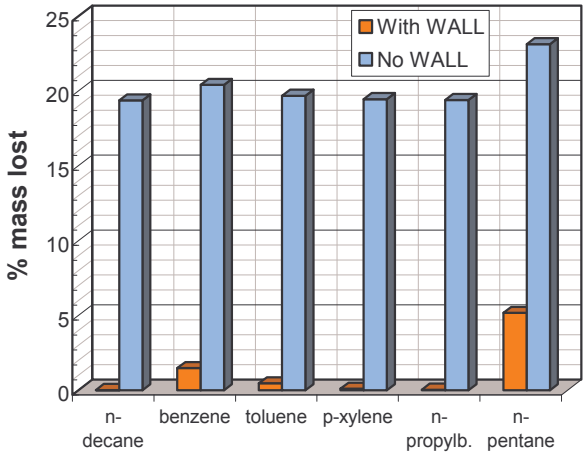

Figure 20. Mass of VOCs lost (%) after 5 years of spill for Cases B and C.

Due to the partinioning of NAPL components into the different phases, the NAPL composition changes, as shown in Figure 21 where the concentration profiles of VOCs in the NAPL at an elevation of -0.25 m asl are plotted as a function of distance from the coast for Case B. The NAPL is depleted upstream of more soluble compounds (benzene, toluene and p-xylene), and consequently is enriched mainly in n-decane and, to a lesser extent, in n-pentane. Downstream, because of n-pentane evaporation, n-pentane is lost with a related increase in n-decane and n-propylbenzene concentrations. These two hydrocarbons are those less affected by partitioning; thus, the weathered NAPL is enriched in these two components.

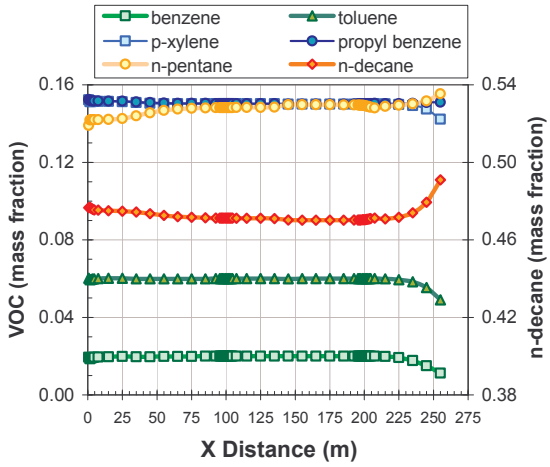

Figure 21. Mass fraction profile of VOCs in the NAPL after 5 years of spill for Case B at -0.25 m asl.

CONCLUSIONS

An improved version of the TMVOC numerical reservoir simulator can be used to model the compositional, multiphase flow of hydrocarbon and organic solvent mixtures spilled in coastal sites, where the sea water intrusion affects the groundwater flow.

The spill of a multi-component mixture of 6 hydrocarbons is simulated using a simple 2D vertical grid orthogonal to the coast line. The spill is simulated both accounting for the sea water intrusion, and for comparative purposes, by assuming a fresh water boundary. The sea water intrusion concentrates the flow of dissolved VOCs in the upper section of the coastal aquifer. This needs to be taken into account if extraction wells are drilled to control the transport of dissolved VOC towards the sea, a measure often requested by controlling authorities. Wells located close to the coast should not be drilled down to the aquifer bottom in order to avoid the unnecessary pumping of sea water, which increases the overall volume of extracted water and determines the progressive advancement of sea water intrusion inside the aquifer.

To demonstrate code capabilities, the effects of the construction of an impervious wall are also simulated and presented. The wall can intercept the NAPL lense avoiding the direct discharge of free NAPL to the sea, while it allows the groundwater to flow beneath it.

The simulations also show how the different characteristics of mixture hydrocarbons and related compositional effects control the VOCs retention in the subsurface and their migration along different pathways. This can be of help for risk assessment studies in sites contaminated by the spill of organic mixtures.

ACKNOWLEDGMENTS

The TMVOC code is based on the PhD research of Adeyinka Adenekan. The improvement of TMVOC V.1 reservoir simulator was performed within the 'Line D - Numerical model', of the ENI R&D project "Clean-up of groundwater and soils contaminated by chlorinated organic solvents" sponsored by the ENI Research Fund.

REFERENCES

Aquater. *Line D - Numerical model*. ENI R&D project "Clean-up of groundwater and soil contaminated by chlorinated organic solvents". Rel_6004, 2003 (*unpublished, in Italian*).

Adenekan, A.E. *Numerical Modeling of Multiphase Transport of Multicomponent Organic Contaminants and Heat in the Subsurface*. PhD thesis, University of California at Berkeley, Berkeley, CA, 1992.

Battistelli, A., C. Calore, K. Pruess. The simulator TOUGH2/EWASG for modelling geothermal reservoirs with brines and a non-condensible gas. *Geothermics, 26(4)*, 437-464, 1997.

Battistelli, A., C.M. Oldenburg, G. Moridis, K. Pruess. Modeling Gas Reservoir Processes with TMVOC V.2.0. Proceedings TOUGH2 Symposium, May 12-14, 2003, Berkeley, CA.

Battistelli, A. Modeling biodegradation of organic contaminants under multiphase conditions with TMVOCBio. *Vadose Zone J., 3(3)*, 875-883, 2004.

Garcia, J.E. *Density of aqueous solutions of CO_2*. Lawrence Berkeley National Laboratory Report LBNL-49023, Berkeley, CA, 2001.

Parker, J.C., R.J. Lenhard, T. Kuppusamy. A Parametric Model for Constitutive Properties Governing Multiphase Flow in Porous Media, *Water Resour. Res.*, 23(4), 618 – 624, 1978.

Oldenburg C.M., K. Pruess. *EOS7R: radionuclide transport for TOUGH2*. Report LBL-34868, Lawrence Berkeley Laboratory, Berkeley, CA, 1995.

Pruess, K. *EOS7 - An equation-of-state module for the TOUGH2 simulator for two-phase flow of saline water and air*. Report LBL-31114, Lawrence Berkeley Laboratory, Berkeley, CA, 1991.

Pruess, K., C.M. Oldenburg, and G. Moridis, *TOUGH2 User's Guide, Version 2.0*, Report LBNL-43134, Lawrence Berkeley National Laboratory, Berkeley, CA, 1999.

Pruess, K. and A. Battistelli. *TMVOC, a Numerical Simulator for Three-Phase Non-Isothermal Flows of Multicomponent Hydrocarbon Mixtures in Saturated-Unsaturated Heterogeneous Media,* Report LBNL-49375, Lawrence Berkeley National Laboratory, 2002.

Reid, R.C., J.M. Prausnitz, and B.E. Poling. *The Properties of Gases and Liquids*, McGraw-Hill, New York, 1987.

Rusi, S., F. Tatangelo, A. Battistelli, E. Crestaz. Density-dependent groundwater modelling for coastal industrial sites. ModelCare 2005, 5th Intl. Conf. on Calibration and Reliability in Groundwater Modelling - From Uncertainty to Decision Making, The Hague June 6-9, 2005.

Sanese, L., A. Battistelli, G. Gottardi. Numerical simulation of organic contaminants migration in coastal aquifers with T2VOC-BRINE. *IGEA,* 18, 65-80, 2003 (*in Italian*).

Stone, H.L. Probability Model for Estimating Three-Phase Relative Permeability. *Trans. SPE of AIME*, 249, 214-218, 1970.